

## **A 2-DIMENSIONAL MODEL COUPLED TO A THERMODYNAMIC DATABASE FOR THE PREDICTION OF SOLIDIFICATION MICROSTRUCTURES IN MULTI-COMPONENT ALLOYS**

A. Jacot<sup>1,2</sup> and Q. Du<sup>1</sup>

<sup>(1)</sup>Laboratoire de Simulation des Matériaux  
Ecole Polytechnique Fédérale de Lausanne  
1015 Lausanne, Switzerland

<sup>(2)</sup> Calcom ESI SA,  
Parc Scientifique, Ecole Polytechnique Fédérale de Lausanne,  
CH-1015 Lausanne, Switzerland.

Keywords: modeling, solidification, microsegregation, aluminum

### **Abstract**

A two-dimensional model for the simulation of microstructure formation during solidification in multi-component systems has been developed. The formation of the primary solid phase is described using a pseudo-front tracking technique. This method permits to calculate the evolution of solid/liquid interfaces which are governed by solute diffusion and anisotropic surface tension. The formation of secondary phases is described with a mixture approach based on the assumption that the interdendritic regions are composed of liquid and secondary phase particles at thermodynamic equilibrium. The model accounts for back-diffusion in the primary phase, which continuously modifies the composition of the interdendritic regions, and for different growth modes. The phase diagram software Thermo-Calc is used to obtain the equilibrium concentrations to be prescribed as boundary conditions at the primary phase/liquid interface and to calculate the phase equilibrium in the interdendritic region during the last stage of solidification. The model has been applied to the description of microstructure formation at different locations in an AA5182 DC casting slab. Comparisons between experimental and calculated microstructures show good agreement.

### **Introduction**

Over the last decade, considerable progress has been made in numerical simulation of solidification microstructures. New models have been proposed for the description of dendritic growth, and in particular, the phase-field method [1,2] emerged as a method of choice to simulate the morphology of the growing solid. One of the major advantages of this technique is to avoid the difficult problem of tracking sharp interfaces in 2 or 3 dimensions, as was done previously in front-tracking models [3]. The pseudo-front tracking methods [4,5,6], which are somewhat in between the phase field and the front-tracking methods, are interesting alternatives to describe solidification at low undercooling and under the assumption of thermodynamic equilibrium at the interface.

Most of the approaches describing dendritic growth in 2 or 3 dimensions are limited to the primary phase formation. On the other hand, many microsegregation models have been proposed to describe the solute distribution and the formation of secondary phases for a

simplified grain geometry [7,8,9,10,11,12]. Simple calculations for the limiting cases of equilibrium (Lever rule) and no diffusion in the solid (Gulliver-Scheil approximation) are available in commercial software such as Thermo-Calc [13] and FactSage [14]. Modifications of the Gulliver-Scheil equation to account for back-diffusion have also been presented in the literature and reviewed in detail in [7]. Some of these models predict the type and amount of secondary phases in multicomponent systems using calculated phase diagrams [8,9,10]. Most of the approaches mentioned here are based on an 1D geometry and are sometimes combined with a coarsening model [11,12].

The objective of the present contribution is to formulate a comprehensive 2-dimensional model which describes first the formation of the primary phase and, in a second stage, the solidification of eutectic or peritectic phases from the remaining interdendritic liquid. The model is based on the two-dimensional pseudo-front tracking method presented in [6], which was extended to describe the secondary phases. The model is coupled to thermodynamic calculations and can be applied to multi-component alloys.

## **Description of the model**

### The primary phase

The model is based on the assumption that the temperature is uniform on the scale of the microstructure and that the phase transformation is governed only by diffusion of the solute element(s) and anisotropic surface tension. The growth of the primary phase ( $\alpha$ ) from the liquid ( $l$ ) is described by solving the diffusion equations in both phases and for all solute species. A solute balance is formulated at the  $\alpha/l$  interface assuming local equilibrium, i.e. the interface concentrations in each phase are deduced from the phase diagram, but accounting for the curvature of the interface.

The solution of the problem is obtained with the pseudo-front tracking method [6] which is based on a finite volume method formulated for a regular hexagonal grid. A volume element or cell of the mesh has three possible states :  $\alpha$ ,  $l$ , or interface  $\alpha/l$ . A layer of interface cells always separates the two phases. An explicit formulation in finite volume method provides a variation of solute concentrations in each cell. For the interfacial cells, these variations correspond to an average over the two phases. Accordingly, the variations of the average concentrations in the interfacial cells are converted into a variation of volume fraction of liquid using a local lever rule, the phase diagram and the local interface curvature. The interface curvature is obtained with the PLIC algorithm which allows the interface to be reconstructed from the knowledge of the solid fraction field [15] and a calculation of the distance field to the interface [6]. Once an interfacial cell is fully transformed, it becomes a solid cell and new interfacial cells are introduced. This procedure diffuses the interface over one mesh size but satisfies the solute flux balance and the equilibrium condition. Further details of the method can be found in [6].

### Secondary phases

As the liquid becomes undercooled for another solid phase, the calculation enters a second stage aimed at predicting the formation of secondary phases in the interdendritic regions. In this approach, the interdendritic regions are considered as a mixture of liquid and solid phases. The following assumptions are made : (i) the composition of the interdendritic liquid is uniform when the first secondary phase starts to form, (ii) the interdendritic region is locally in

thermodynamic equilibrium and all phases have uniform concentrations, (iii) back diffusion affects the interdendritic region in a uniform manner.

A solute balance is performed over the interdendritic domain,  $\Omega_m$ , for all the solute elements :

$$\int_{\Gamma_{\alpha/m}} \mathbf{J}_i^\alpha \cdot \mathbf{n} \, d\Gamma = \int_{\Omega_m} \frac{\partial w_i^m}{\partial t} \, d\Omega - \int_{\Gamma_{\alpha/m}} (w_i^m - w_i^\alpha) \mathbf{v} \cdot \mathbf{n} \, d\Gamma \quad i=1, n \quad (1)$$

where  $n$  is the number of solutes,  $\mathbf{J}_i^\alpha$  is the back-diffusion flux of element  $i$ ,  $w_i^\alpha$  is the equilibrium concentration of element  $i$  in  $\alpha$  at the interface,  $w_i^m$  is the average concentration of element  $i$  in the interdendritic region,  $\Gamma_{\alpha/m}$  is the contour of the  $\alpha/m$  interface which separates the primary phase and the interdendritic region,  $\mathbf{v}$  is the velocity of the  $\alpha/m$  interface and  $\mathbf{n}$  is the normal vector to  $\Gamma_{\alpha/m}$  pointing toward  $\Omega_m$ .

Introducing  $\Phi_i^\alpha = \int_{\Gamma_{\alpha/m}} \mathbf{J}_i^\alpha \cdot \mathbf{n} \, d\Gamma$  and discretizing (1), we obtain :

$$\Phi_i^\alpha \delta t = V_m \delta w_i^m + \delta V_m (w_i^m - w_i^\alpha) \quad i=1, n \quad (2)$$

where  $V_m$  is the volume of  $\Omega_m$  and the symbol  $\delta$  expresses small increments.

The mixture composition can be expressed as :

$$w_i^m = \sum_{\nu=1}^p g_\nu w_i^\nu \quad i=1, n \quad (3)$$

where  $p$  is the number of phases in the mixture,  $w_i^m$  is the equilibrium concentration of element  $i$  in phase  $\nu$  and  $g_\nu$  is the volume fraction of phase  $\nu$  in the interdendritic region.

Assuming that thermodynamic equilibrium is satisfied, the temperature can be related to the phase diagram :

$$T = T^{\alpha/\nu} (w_1^\alpha, \dots, w_n^\alpha) \quad \forall \nu \neq \alpha \quad (4)$$

where  $T^{\alpha/\nu}(w_1^\alpha, \dots, w_n^\alpha)$  expresses the solidus (or solvus) temperature as a function of the concentration in  $\alpha$ .

The concentrations of the other phases are given by the tie-lines :

$$w_i^\nu = k_i^{\nu/\alpha} (w_1^\alpha, \dots, w_n^\alpha) w_i^\alpha \quad \forall \nu \neq \alpha \quad i=1, n \quad (5)$$

where the  $k_i^{\nu/\alpha}$  are partition coefficients defined with respect to  $\alpha$ .

The back-diffusion contribution,  $\Phi_i^\alpha$ , is calculated with the explicit finite volume method already used in the primary phase calculation. Assuming that the thermal history is known, the evolution of the system can be described by the following set of equations :

$$\Phi_i^\alpha \delta t = V_m \left( \sum_{\nu=1}^p \delta g_\nu w_i^\nu + \sum_{\nu=1}^p g_\nu \delta w_i^\nu \right) + \delta V_m \left( \left( \sum_{\nu=1}^p g_\nu w_i^\nu \right) - w_i^\alpha \right) \quad i=1, n \quad (6)$$

$$\sum_{\nu=1}^p \delta g_\nu = 0 \quad (7)$$

$$T + \delta T = T^{\nu/\alpha} (w_1^\alpha + \delta w_1^\alpha, \dots, w_n^\alpha + \delta w_n^\alpha) \quad \nu \neq \alpha \quad (8)$$

$$w_i^\nu + \delta w_i^\nu = k_i^{\nu/\alpha} (w_1^\alpha + \delta w_1^\alpha, \dots, w_n^\alpha + \delta w_n^\alpha) (w_i^\alpha + \delta w_i^\alpha) \quad \nu \neq \alpha \quad (9)$$

Equation (6) to (9) form a set of  $p(n+1)$  equations which comprises  $1+p(n+1)$  unknowns : the  $\{\delta w_i^v\}$ , the  $\{\delta g_v\}$  and  $\delta V_m$ . The following equation is appended to the system in order to close the problem :

$$\lambda = \frac{\delta V_m}{\delta V_m + \delta g_\alpha V_m} \quad (10)$$

This equation expresses the proportion of  $\alpha$  phase formed on the  $\alpha/m$  interface with respect to the amount formed within the interdendritic region. By selecting an appropriate value for  $\lambda$ , it is possible to distinguish the behaviors of divorced and coupled eutectics. If  $\lambda$  is set to 1 (i.e.,  $\delta g_\alpha = 0$ ),  $\alpha$  will form only on top of the primary phase (divorced eutectics), whereas for  $\lambda = 0$  ( $\delta V_m = 0$ ) it will be distributed in the interdendritic region and the primary phase boundaries will remain stationary (coupled eutectics).

### Thermodynamic data

The thermodynamic data needed for the calculation, i.e. the liquidus temperatures and the partition coefficients are obtained with thermodynamic calculation based on the commercial package Thermo-Calc [13]. An optimization strategy has been developed in order to reduce the number of thermodynamic calculations. The approach is based on the assumption that the differences between the interfacial concentrations within the calculation domain can be approximated by linear functions. More precisely, the liquidus temperature and the partition coefficients are calculated with linear functions of the deviation from the average concentrations at the interface. At each time step,  $(n+1)$  equilibrium calculations are performed in order to update the parameters of the linear functions, i.e., the liquidus and partition coefficients for the average interface cell and, the partial derivatives with respect to each of the  $n$  solute elements. A few additional calculations are needed to test the stability of the secondary phases.

## **Results and Discussion**

The model was used to simulate the microstructure formation at various locations in a DC casting AA5182 aluminum slab which was produced vertically in an 1880 mm x 510 mm section mould at a pulling speed of 60 mm/min. The slab was instrumented with 6 thermocouples positioned at 27, 53, 93, 144, 198 and 253 mm from the rolling face. Samples were taken at each location for metallographic analysis. The type and the amount of secondary phases were measured by EDX and image analysis.

The measured cooling curves which are presented in Fig. 1 were used as a thermal input for microstructure calculations at the corresponding locations. The calculations were performed using a nominal composition of 0.22wt%Fe, 4.30wt%Mg, 0.33wt%Mn, 0.11wt%Si. Solid seeds were nucleated randomly in the computational domain using a grain density estimated from the micrographs. The dimensions of the domain were chosen in order to have between 4 and 10 grains in the domain. The simulated microstructure obtained for the 27 mm location is presented in Fig. 2 where the different grey levels indicate the local Mg concentration. The microstructure can be compared with the micrograph of the corresponding sample in Fig. 3, recalling that the density of solid seeds introduced in the calculation domain was determined from this micrograph.

Fig. 1 : measured cooling curves at various distances from the rolling face in the AA5182 DC casting slab.

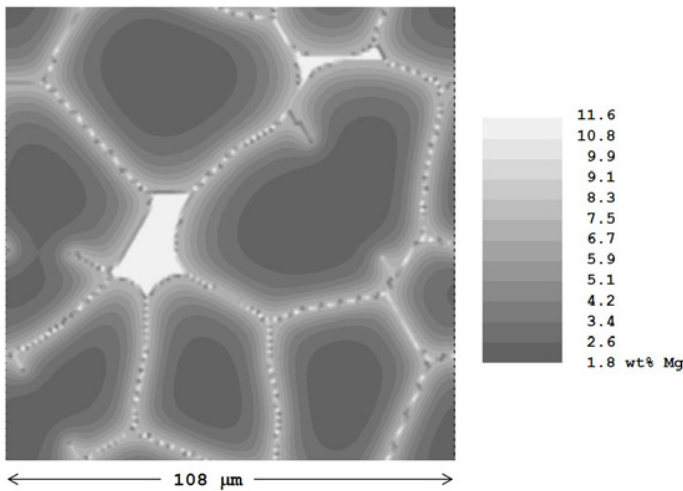
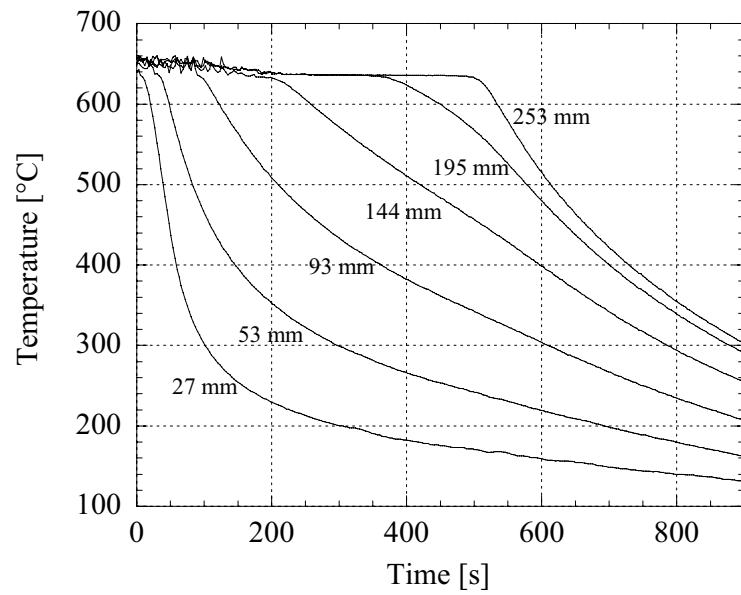


Fig. 2 : calculated Mg concentration field at 27 mm from the rolling face.

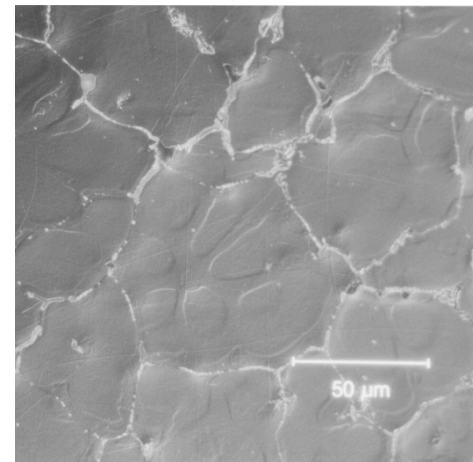
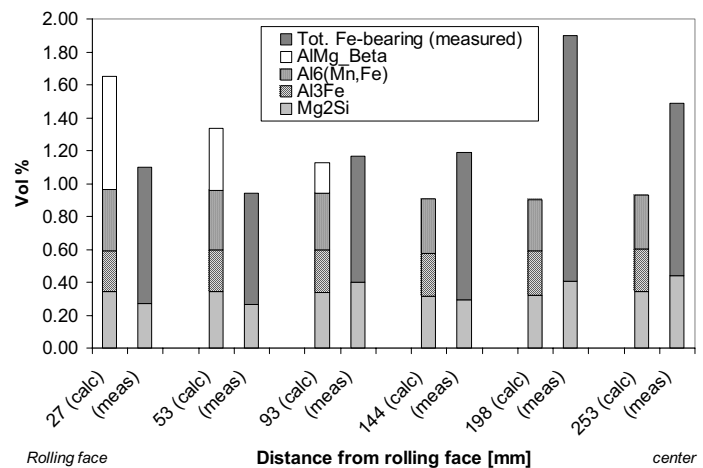


Fig. 3 : microstructure at 27 mm from the rolling face.

Fig. 4 : calculated and measured volume fractions of phases at various distances from the rolling face in the AA5182 DC casting slab.



Four types of secondary phases are predicted with the model :  $Mg_2Si$ ,  $Al_3Fe$ ,  $Al_6(Mn,Fe)$  and  $AlMg-\beta$ . Their volume percentage is presented in Figure 4, together with the experimental area fractions. For the first four positions (27, 53, 93 and 144 mm), the volume fractions of  $Mg_2Si$  and the cumulated fractions of  $Al_3Fe$  and  $Al_6(Mn,Fe)$  calculated with the model are in good agreement with the corresponding measured amounts. The differences fall within the experimental error, which was estimated to 20%. The model predicts also the formation of  $AlMg-\beta$  close to the surface. Unfortunately comparison with experiment is not possible for this phase due to difficulties in measuring the area fraction. However, the presence of  $AlMg-\beta$  has been identified by EDX. Close to the centerline (198 and 253 mm), some discrepancy is observed between simulation and observation, namely in the amount of Fe-bearing particles, which is substantially smaller in the simulation than in the measurement. This discrepancy is believed to be due to macrosegregation, which is commonly observed in the center region of DC casting slabs. Other possible reasons which might be invoked are the accuracy of the data used in the calculations (diffusion coefficients and thermodynamic data) and the assumptions of the model (uniform liquid during secondary phase formation, negligible nucleation undercooling of secondary phases, thermodynamic equilibrium). However, since good agreement is obtained for the other locations it is believed that these issues may not completely explain the discrepancy. Further investigations are underway to confirm the influence of macrosegregation.

### **Conclusion**

A numerical model for the description of microstructure formation during solidification of multi-component systems has been developed. A pseudo-front tracking technique is used to describe the evolution of the solid/liquid interface, assuming it is governed by solute diffusion and the Gibbs-Thomson effect. The formation of the secondary phases is described with a mixture approach based on the assumption that the interdendritic regions are in thermodynamic equilibrium. The model was coupled to a thermodynamic database using a computationally efficient strategy based on direct calls to Thermo-Calc. The pseudo-front tracking model was used successfully to describe the type and the amount of secondary phases in a quinary commercial aluminum alloy. The present model provides an interesting tool to study the influence of alloy composition, casting conditions and inoculation on the resulting microstructure, microsegregation profiles and interdendritic phases.

### **Acknowledgements**

This research was carried out as part of the Fifth Framework Competitive and Sustainable Growth program project GRD1-1999-10921 VIRCAST (Contract N° G5RD-CT-2000-00153). It included the partners: Alcan (Switzerland), Calcom-ESI (Switzerland), Elkem Aluminum (Norway), École Polytechnique Fédérale de Lausanne (Switzerland), Corus (The Netherlands), Hydro Aluminum (Norway), Hydro Aluminum (Germany), Institute National Polytechnique de Grenoble (France), Institute National Polytechnique de Lorraine (France), Norwegian University of Science and Technology (Norway), Péchiney S.A. (France), and IFE (Norway) and SINTEF (Norway), as major subcontractors. Funding by the European Community and by the Office Fédéral de l'Éducation et de la Science (Bern) is gratefully acknowledged. The authors would like to address special thanks to Ph. Gilgien (Alcan) and E. Jenssen (Elkem) for providing the experimental data.

## References

1. W. J. Boettinger, J. A. Warren, C. Beckermann, A. Karma, *Annu. Rev. Mater. Res.* **32**, 163-94 (2002).
2. L. Q. Chen, *Annu. Rev. Mater. Res.*, **32**, 113-140 (2002).
3. Y. Saito, G. Goldbeck-Wood and H. Muller-Krumbhaar, "Numerical Simulation of Dendritic Growth", *Physical Review A*, **38**, 2148-2157 (1988).
4. U. Dilthey and V. Pavlik, in *Modeling of Casting and Advanced Solidification Processes VIII*, ed. by B. G. Thomas and C. Beckermann, TMS, p. 589 (1998).
5. D. Juric and G. Tryggvason, *J. of Computational Physics*, **123**, 127 (1996).
6. A. Jacot and M. Rappaz, *Acta mater.*, **50**, 1909-1926 (2002).
7. T. Kraft and Y.A. Chang, Predicting Microstructure and Microsegregation in Multicomponent Alloys, *Journal of Metals*, **47**, 20-28 (1997).
8. W. Yamada, T. Matsumiya and A. Ito, Proceedings of the 6th International Iron and Steel Congress, 1990, The Iron and Steel Institute of Japan, Tokyo, pp. 618.
9. U.R. Kattner, W.J. Boettinger and S.R. Coriell, *Z. Metallkde.*, **87**, 522-528 (1996).
10. X. Doré, H. Combeau and M. Rappaz, *Acta mater.*, **48**, 3951-3962 (2000).
11. V.R. Voller and C. Beckermann, *Met. Trans.*, **30A**, 2183-2189 (1999).
12. T. Kraft, M. Rettenmayr and H.E. Exner, *Modelling Simul. Mater. Sci. Eng.*, **4**, 161-177 (1996).
13. B. Sundman, B. Jansson and J.O. Andersson, *CALPHAD*, **9**, 153-190 (1985).
14. G. Eriksson, *GTT CHEMSAGE Handbook*, Version 3.0.1 (GTT-Technologies, Kaiserstr. 100, D-52134, Herzogenrath, 1994).
15. D.B. Kothe, W.J. Rider, S.J. Mosso and J.S. Brock, internal report, Los Alamos Laboratories (1996).